

Theoretical Study on the Assembly and Stabilization of a Silicon-Doped All-Metal Aromatic Unit SiAl_3^-

Li-ming Yang, Jian Wang, Yi-hong Ding,* and Chia-chung Sun

State Key Laboratory of Theoretical and Computational Chemistry, Institute of Theoretical Chemistry, Jilin University, Changchun 130023, People's Republic of China

Received May 15, 2007

We predict the assembly and stabilization of the silicon-doped all-metal aromatic unit SiAl_3^- based on the density functional calculations on a series of model compounds $[\text{D}(\text{SiAl}_3)\text{M}]^{q-}$ as well as the saturated compounds $[\text{D}(\text{SiAl}_3)\text{M}_n]$ ($\text{D} = \text{SiAl}_3^-, \text{Cp}^-(\text{C}_5\text{H}_5^-)$; $\text{M} = \text{Li, Na, K, Be, Mg, Ca}$) and the more extended sandwich-like species. For all six metals, SiAl_3^- can be assembled only in “heterodecked sandwich” scheme (e.g., $[\text{CpM}(\text{SiAl}_3)]^{q-}$) so as to avoid cluster fusion. Interestingly, among all the designed sandwich species, SiAl_3^- generally prefers to interact with the partner deck at the side (Al–Al or Al–Si bonds) or corner (Si or Al atoms) site, in contrast to the known decks such as $\text{Cp}^-, \text{P}_5^-, \text{N}_4^{2-}$, and Al_4^{2-} , which take the traditional face–face interaction type. Such interaction types present an interesting growth pattern that might be applicable to the assembly of Si-doped all-metal aromatic SiAl_3^- units into highly extended sandwich complexes. Our results for the first time showed that the electronic, structural, and aromatic properties of the silicon-doped all-metal aromatic SiAl_3^- could be well-retained during cluster assembly.

1. Introduction

“Aromaticity” in organic compounds has been one of the most important concepts in chemistry for more than a century. The unexpected observation of the square-planar Al_4^{2-} unit in bimetallic compounds MAl_4^- ($\text{M} = \text{Li, Na, Cu}$) by Li et al. in 2001 has led to the concept of “aromaticity” in the all-metal species.¹ Many of these aromatic species, such as XAl_3^- ($\text{X} = \text{Si, Ge, Sn, Pb}$),² M_4^{2-} ($\text{M} = \text{Ga, In, Tl, Sb, Bi}$),^{3–5} M_4^{2+} ($\text{M} = \text{Se, Te}$),⁶ M_3^- ($\text{M} = \text{Al, Ga}$),⁷ Al_6^{2-} ,⁸ Hg_4^{6-} ,⁹ M_5^{6-} ($\text{M} = \text{Ge, Sn, Pb}$),¹⁰ M_5^- ($\text{M} = \text{Sb, Bi}$),^{11,12} Au_5Zn^+ ,¹³ Cu_3^{3+} ,¹⁴ Cu_4^{2-} ,¹⁵ and $[\text{Fe}(\text{X}_5)]^+$ ($\text{X} = \text{Sb, Bi}$),¹⁶ have now joined the growing all-metal aromatic family.¹⁷ These species are usually electron-

deficient and possess large resonance stabilization energies,¹⁸ which is ascribed to the “multiple aromaticity” feature.¹⁸ Because of their interesting chemical structures, bonding properties, and potential application in material science, it is no surprise that the all-metal aromatic species have received very extensive attention in various aspects, i.e., fundamental study¹⁷ and application research.¹⁷ Interestingly, the experimental identification of some species (e.g., Al_3^- and Hg_4^{6-}) was earlier than the milestone Al_4^{2-} . In particular, Hg_4^{6-} already existed in ancient amalgams!¹⁹ It is thus reasonable to state that the all-metal aromatic molecules have played and will continue to play an important role in novel materials science. The further and ultimate goal is surely to design novel one-dimensional (1D), two-dimensional (2D), and three-dimensional (3D) cluster-assembled materials based on the concept of “all-metal aromaticity”. Yet, as Kuznetsov et al. stated,⁸ “...the question remains if the X_4^{2-} aromatic rings can be incorporated into sandwich-type complexes...” ($\text{X} = \text{Al, Ga, In}$). We feel that such issues should also exist for the assembly of other all-metal aromatic species.

* Author to whom correspondence should be addressed. E-mail: yhdd@mail.jlu.edu.cn.

(1) (a) Li, X.; Kuznetsov, A. E.; Zhang, H. F.; Boldyrev, A. I.; Wang, L. S. *Science* **2001**, *291*, 859. (b) Ritter, S. K. *Chem. Eng. News* **2001**, *79* (39), 39.

(2) Li, X.; Zhang, H. F.; Wang, L. S.; Kuznetsov, A. E.; Cannon, N. A.; Boldyrev, A. I. *Angew. Chem., Int. Ed.* **2001**, *40*, 1867.

(3) Kuznetsov, A. E.; Boldyrev, A. I.; Li, X.; Wang, L. S. *J. Am. Chem. Soc.* **2001**, *123*, 8825–8831.

(4) Twamley, B.; Power, P. P. *Angew. Chem., Int. Ed.* **2000**, *39*, 3500.

(5) (a) Cisar, A.; Corbett, J. D. *Inorg. Chem.* **1977**, *16*, 2482. (b) Critchlow, S. C.; Corbett, J. D. *Inorg. Chem.* **1984**, *23*, 770. (c) Tuononen, H. M.; Suontamo, R.; Valkonen, J.; Laitinen, R. S. *J. Phys. Chem. A* **2004**, *108*, 5670.

(6) (a) Gillespie, R. J.; Barr, J.; Kapoor, R.; Malhotra, K. C. *Can. J. Chem.* **1968**, *46*, 149. (b) Gillespie, R. J.; Barr, J.; Crump, D. B.; Kapoor, R.; Ummat, P. K. *Can. J. Chem.* **1968**, *46*, 3607. (c) Barr, J.; Gillespie, R. J.; Kapoor, R.; Pez, G. P. *J. Am. Chem. Soc.* **1968**, *90*, 6855. (d) Couch, T. W.; Lokken, D. A.; Corbett, J. D. *Inorg. Chem.* **1972**, *11*, 357. (e) Burford, N.; Passmore, J.; Sanders, J. C. P. In *From Atoms to Polymers. Isoelectronic Analogies*; Liebman, J. F., Greenburg, A., Eds.; VCH: New York, 1989; pp 53–108.

(7) (a) Li, X.; Wang, X. B.; Wang, L. S. *Phys. Rev. Lett.* **1998**, *81*, 1909. (b) Wu, H.; Li, X.; Wang, X. B.; Ding, C.-F.; Wang, L. S. *J. Chem. Phys.* **1998**, *109*, 449. (c) Baeck, K. K.; Bartlett, R. J. *J. Chem. Phys.* **1998**, *109*, 1334. (d) Kuznetsov, A. E.; Boldyrev, A. I. *Struct. Chem.* **2002**, *13*, 141.

(8) Kuznetsov, A. E.; Boldyrev, A. I.; Zhai, H.-J.; Li, X.; Wang, L.-S. *J. Am. Chem. Soc.* **2002**, *124*, 11791.

(9) (a) Nielsen, J. W.; Baenziger, N. C. *Acta Crystallogr.* **1954**, *7*, 277. (b) Corbett, J. D. *Inorg. Nucl. Chem. Lett.* **1969**, *5*, 81. (c) Kuznetsov, A. E.; Corbett, J. D.; Wang, L. S.; Boldyrev, A. I. *Angew. Chem. Int. Ed.* **2001**, *40*, 3369.

(10) (a) Todorov, I.; Sevov, S. C. *Inorg. Chem.* **2004**, *43*, 6490. (b) Todorov, I.; Sevov, S. C. *Inorg. Chem.* **2005**, *44*, 5361.

(11) (a) Gausa, M.; Kaschner, R.; Lutz, H. O.; Seifert, G.; Meiwes-Broer, K.-H. *Chem. Phys. Lett.* **1994**, *230*, 99. (b) Gausa, M.; Kaschner, R.; Seifert, G.; Faehrmann, J.-H.; Lutz, H. O.; Meiwes-Broer, K.-H. *J. Chem. Phys.* **1996**, *104*, 9719.

(12) Zhai, H. J.; Wang, L. S.; Kuznetsov, A. E.; Boldyrev, A. I. *J. Phys. Chem. A* **2002**, *106*, 5600.

(13) Tanaka, H.; Neukermans, S.; Janssens, E.; Silverans, R. E.; Lievens, P. *J. Am. Chem. Soc.* **2003**, *125*, 2862.

(14) Alexandrova, A. N.; Boldyrev, A. I.; Zhai, H.-J.; Wang, L. S. *J. Phys. Chem. A* **2005**, *109*, 562.

(15) Wannere, C. S.; Corminboeuf, C.; Wang, Z.-X.; Wodrich, M. D.; King, R. B.; Schleyer, P. v. R. *J. Am. Chem. Soc.* **2005**, *127*, 5701.

(16) Lein, M.; Frunzke, J.; Frenking, G. *Angew. Chem., Int. Ed.* **2003**, *42*, 1303.

(17) (a) Boldyrev, A. I.; Wang, L. S. *Chem. Rev.* **2005**, *105*, 3716–3757, and references therein. (b) Tspis, C. A. *Coord. Chem. Rev.* **2005**, *249*, 2740–2762, and references therein.

(18) Zhan, C.-G.; Zheng, F.; Dixon, D. A. *J. Am. Chem. Soc.* **2002**, *124*, 14795.

Doping is a very important technique in cluster and materials science. We are aware that some heterodoped all-metal aromatic species have been experimentally observed.² As a basic step toward understanding the doping effects of the assembly of the all-aromatic units that might be utilized in the future, we made an attempt to assemble a heterodoped all-metal aromatic unit. The Si-doped all-metal aromatic unit SiAl_3^{-2} is taken for our model design. Here we consider an important and widely applied strategy, “sandwiching”, which is probably the most powerful one for the assembly of a stable unit (e.g., C_5H_5^- (Cp^-)) into molecular materials and has gestated a rich chemistry of metallocenes (Cp_2M).¹⁹ It is known that in traditional metallocenes (Cp_2M) the interaction between the metal atom and the sandwiching unit is mainly ionic. It is thus reasonable to expect that the monoanionic SiAl_3^- deck should also preferentially interact with the metal atom via ionic interaction. In addition, the lower electronic negativity of alkali elements Li, Na, and K and alkaline-earth Be, Mg, and Ca make them likely to form ionic interactions, which makes alkali and alkaline-earth metals good candidates to test the ionic interaction of the SiAl_3^- deck in the sandwich-like complexes. We found that for all six metals, $\text{M} = \text{Li}, \text{Na}, \text{K}, \text{Be}, \text{Mg}, \text{and Ca}$, the assembly of SiAl_3^- cannot be realized in the traditional “homodecked sandwich” form $[(\text{SiAl}_3)_2\text{M}]^{q-}$. However, our recently proposed “heterodecked sandwich” scheme²⁰ (e.g., $[\text{CpM}(\text{SiAl}_3)]^{q-}$) is very effective in assembly. The good structural and electronic integrity of the SiAl_3^- unit within the designed assembly systems leads us to propose that the all-metal aromatic SiAl_3^- might act as a building block or inorganic ligand in cluster-assembled molecular compounds.

2. Computational Methods

Initially, we fully optimized the geometries of $[\text{D}(\text{SiAl}_3)\text{M}]^{q-}$ ($\text{D} = \text{SiAl}_3^-, \text{Cp}^-$; $\text{M} = \text{Li}, \text{Na}, \text{K}, \text{Be}, \text{Mg}, \text{Ca}$) by employing analytical gradients with a polarized split-valence basis set (6-311+G(d))²¹ and using the hybrid method, which includes a mixture of Hartree–Fock exchange and density functional exchange correlation (B3LYP),²² as implemented in Gaussian 03.²³ After geometrical optimization, normal mode vibrational analysis was

(19) (a) Peckham, T. J.; Gomez-Eliphe, P.; Manners, I. *Metallocenes*; Togni, A., Halterman, R. L., Eds.; Wiley-VCH: Weinheim, 1998; Vol. 2, p 724. (b) Togni, A., Halterman, R. L., Eds. *Metallocenes: Synthesis, Reactivity, Applications*; Wiley-VCH: Weinheim, Germany, 1998.

(20) Note that there are other papers in the literature using somewhat similar structural motifs. For example see: (a) Tremel, W.; Hoffmann, R.; Kertesz, M. *J. Am. Chem. Soc.* **1989**, *111*, 2030, and reference therein. (b) Scherer, O. J.; Bruck, T. *Angew. Chem.* **1987**, *99*, 59; *Angew. Chem., Int. Ed. Engl.* **1987**, *26*, 59. (c) Frunzke, J.; Lein, M.; Frenking, G. *Organometallics* **2002**, *21*, 3351–3359. (d) Padma, E. J. Malar. *Eur. J. Inorg. Chem.* **2004**, 2723–2732. (e) We are aware that another possibility is to apply a “heteroleptic sandwich”; see: Merino, G.; Beltran, H.; Vela, A. *Inorg. Chem.* **2006**, *45*, 1091–1095. A “heterodecked sandwich” scheme was newly proposed and successfully applied in our previous work. (f) Yang, L. M.; Ding, Y. H.; Sun, C. C. *Chem. Phys. Chem.* **2006**, *7*, 2478–2482. (g) Yang, L. M.; Ding, Y. H.; Sun, C. C. *Chem.–Eur. J.* **2007**, *13*, 2546–2555. (h) Yang, L. M.; Ding, Y. H.; Sun, C. C. *J. Am. Chem. Soc.* **2007**, *129*, 658–665. (i) Yang, L. M.; Ding, Y. H.; Sun, C. C. *J. Am. Chem. Soc.* **2007**, *129*, 1900–1901.

(21) (a) McLean, A. D.; Chandler, G. S. *J. Chem. Phys.* **1980**, *72*, 5639–5648. (b) Clark, T.; Chandrasekhar, J.; Spitznagel, G. W.; Schleyer, P. v. R. *J. Comput. Chem.* **1983**, *4*, 294–299. (c) Frisch, M. J.; Pople, J. A.; Binkley, J. S. *J. Chem. Phys.* **1984**, *80*, 3265–3269.

(22) (a) Parr, R. G.; Yang, W. *Density-Functional Theory of Atoms and Molecules*; Oxford University Press: Oxford, 1989. (b) Becke, A. D. *J. Chem. Phys.* **1992**, *96*, 2155–2160. (c) Perdew, J. P.; Chevary, J. A.; Vosko, S. H.; Jackson, K. A.; Pederson, M. R.; Singh, D. J.; Fiolhais, C. *Phys. Rev. B* **1992**, *46*, 6671–6687.

(23) Frisch, M. J.; et al. *Gaussian03* (Revision A.1); Gaussian, Inc.: Pittsburgh, PA, 2003. (For a full citation of Gaussian03 see the Supporting Information.)

performed to check whether the obtained structure is a true minimum point with all real frequencies or a first-order transition state with only one imaginary frequency. Despite its widespread use, aromaticity is more a concept rather than a directly measurable quantity. Consequently, measurements of aromaticity rely on many diverse criteria.²⁴ Among them, the nucleus-independent chemical shift (NICS), based on the “absolute magnetic shielding” taken at the center of a ring compound, is widely used and has been proven to be accurate for ordinary cyclic carbon compounds.²⁵ Recently this method has also been successfully used for inorganic cyclic aromatic compounds,²⁶ including the characterization of the so-called d-orbital aromaticity.²⁷ Thus, the NICS values were also calculated at the B3LYP/6-311+G(d) level of theory. A positive value of the NICS indicates that the molecule is antiaromatic; a negative value indicates the aromaticity of the molecule. The NICS calculated at the center of the square (NICS(0)) describes the σ aromaticity, and the NICS more than 1 Å out of the square plane (NICS(1)) describes the π aromaticity of the molecule. All the calculations were performed with the Gaussian-03 program.²³

3. Theoretical Results and Discussion

Our research takes the following scheme: model sandwich species (singly or multiply charged anions), saturated sandwich species (with counterions), and extended sandwich species. Such a scheme has been applied to many charged systems. In a number of cases, the B3LYP method has been proved to be cost-effective, saves on disk space, and is reliable in predicting structures and energetics. The successful applications of the B3LYP method by our own and other groups motivated us to perform the B3LYP/6-311+G(d) calculations for the present system in a systematic way.

In order to get insight into the sandwich-type interaction forms, here, we make some additional interpretations on the sandwich-type interactions. We are aware that the usual definition of the traditional sandwich-type compounds, of which the two decks are parallel rings (e.g., FeCp_2 ,^{28a} CrBz^{28b}), was formed after the discovery of ferrocenes (FeCp_2)^{28a} and dibenzene chromium (CrBz_2).^{28b} After analyzing various sandwich-like compounds and interaction forms, we think that the definition of sandwich compounds should not be limited to the forms of the parallel rings. Sloped sandwich-type forms Cp_2X ($\text{X} = \text{C}, \text{Si}$) have been known for a long time. Thus, we propose that the sandwich compounds are the interactions of the deck–core–deck in various forms. The decks can be organic, inorganic, all-metal, homocyclic, and heterocyclic ligands, etc. The cores can be not only transition-metal but also main-group-metal and nonmetal atoms. The coordination number of the ligand in the sandwich compounds could be η^1 – η^8 . The beryllocene BeCp_2 ²⁹ adopts an η^5/η^1 slip-sandwich structure, which is very similar to the face–corner (f-c) sandwich-type forms of $[\text{CpM}(\text{SiAl}_3)]^{q-}$.

(24) Minkin, V. I.; Glukovtsev, M. N.; Simkin, B. Y. *Aromaticity and Antiaromaticity*; Wiley: New York, 1994.

(25) Chen, Z.; Wannere, C. S.; Corminbeouf, C.; Puchta, R.; Schleyer, P. v. R. *Chem. Rev.* **2005**, *105*, 3842–3888.

(26) (a) Chen, Z.; Corminbeouf, C.; Heine, T.; Bohmann, J.; Schleyer, P. v. R. *J. Am. Chem. Soc.* **2003**, *125*, 13930–13931. (b) Jung, Y.; Heine, T.; Schleyer, P. v. R.; Head-Gordon, M. *J. Am. Chem. Soc.* **2004**, *126*, 3132–3138.

(27) (a) Tsipis, A. C.; Tsipis, C. A. *J. Am. Chem. Soc.* **2003**, *125*, 1136–1137. (b) Tsipis, C. A.; Karagiannis, E. E.; Kladou, P. F.; Tsipis, A. C. *J. Am. Chem. Soc.* **2004**, *126*, 12916–12929. (c) Huang, X.; Zhai, H. J.; Kiran, B.; Wang, L. S. *Angew. Chem.* **2005**, *117*, 7417–7420; *Angew. Chem., Int. Ed.* **2005**, *44*, 7251–7254. (d) Corminbeouf, C. S.; Wannere, C. S.; Roy, D.; King, R. B.; Schleyer, P. v. R. *Inorg. Chem.* **2006**, *45*, 214–219.

(28) (a) Kealy, T. J.; Pauson, P. L. *Nature* **1951**, *168*, 1039. (b) Fischer, E. O.; Hafner, W. Z. *Naturforsch.* **1955**, *10B*, 665.

(29) Almenningen, A.; Haaland, A.; Luszyk, J. J. *Organomet. Chem.* **1979**, *170*, 271.

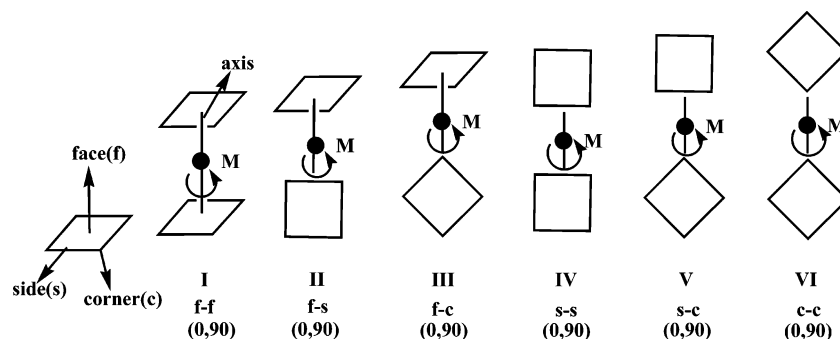


Figure 1. Six possible sandwich types of $[(\text{SiAl}_3)_2\text{M}]^{q-}$ (I–VI) for each M. In each type, one unit can rotate along the axis by 0° and 90° . Moreover, Si and Al atoms can be exchanged in each type.

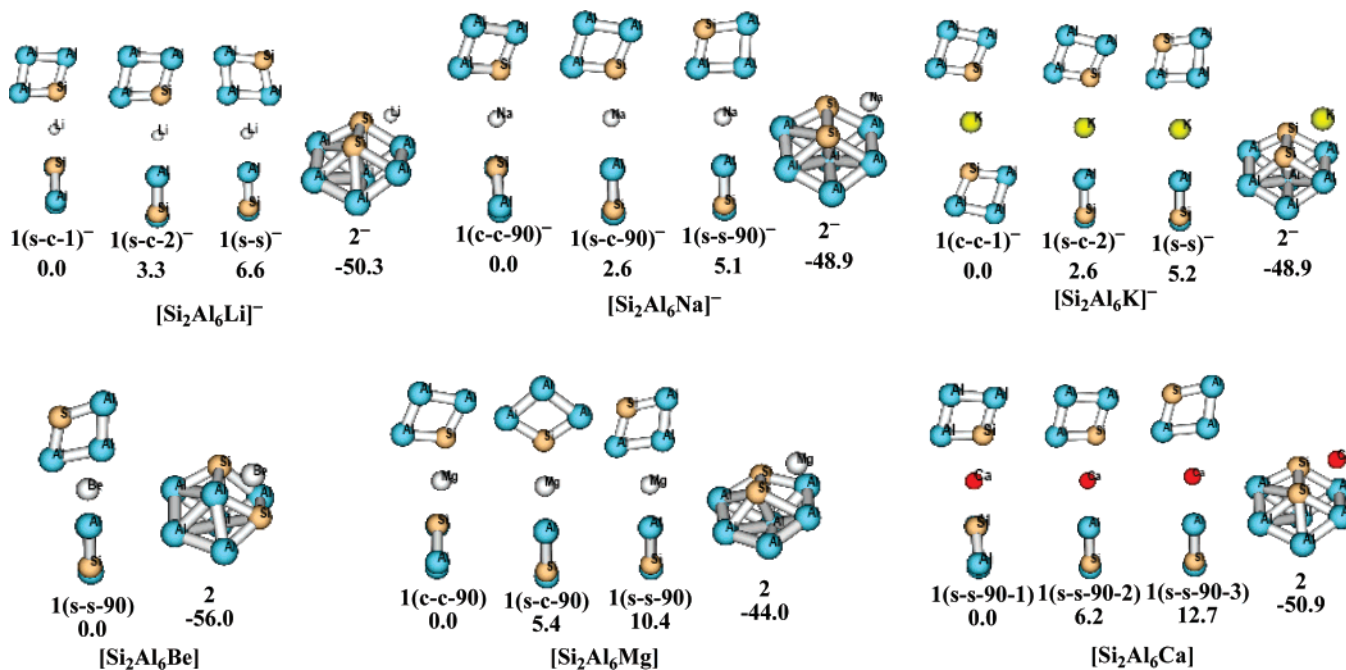


Figure 2. Most relevant $[\text{Si}_2\text{Al}_6\text{M}]^{q-}$ ($\text{M} = \text{Li}, \text{Na}, \text{K}, q = 1$; $\text{M} = \text{Be}, \text{Mg}, \text{Ca}, q = 0$) species obtained at the B3LYP/6-311+G(d) level. The energy values are in kcal/mol.

So, our original redefinition of sandwich compounds has a basis in traditional metallocenes.

On the other hand, some oligomeric and polymeric metallocenes existent in the crystal solid have been known for a long time. Our designed extended structures are very similar to the cyclopentadienyl-element clusters³⁰ (e.g., see ref 30, Figure 3, refs 17 and 18) or oligomeric cyclopentadienyl-element complexes. Thus, we can view our designed extended structures as extended sandwich-like compounds (just like the extended sandwich-like compounds in our previous work; e.g., see refs 20h,i).

Homodecked Sandwich-Type Compounds: $[(\text{SiAl}_3)_2\text{M}]^{q-}$.

As a model calculation, we first investigated the assembly of the all-metal aromatic SiAl_3^- in the traditional “homodecked sandwich” form $[(\text{SiAl}_3)_2\text{M}]^{q-}$ with $\text{M} = \text{Li}, \text{Na}, \text{K}, q = 1$; $\text{M} = \text{Be}, \text{Mg}, \text{Ca}, q = 0$ at the B3LYP/6-311+G(d) level. The possible sandwich types are shown in Figure 1. The type I structure is similar to the well-known metallocenes Cp_2M , in which two Cp^- adopt the face–face (f-f) type. After a detailed structural search at the B3LYP/6-311+G(d) level, the energy profiles of the most relevant $[\text{Si}_2\text{Al}_6\text{M}]^{q-}$ species, i.e., all

sandwich forms and the lowest-energy fusion forms, are schematically shown in Figure 2. The other isomers can be found in the Supporting Information (SI). First, for all six main-group metal elements, the sandwich species IV, V, and VI have very close energies to each other and are all energetically lower than I, II, and III. Via the rotation of the SiAl_3 deck along different axes, I–III can be easily converted to the lower-energy IV–VI. The interconversion between IV and VI via simple rotation is also very easy, which can be indicated by the very small rotation frequency. Second, from Figure 2, we can see that the lowest-energy sandwich isomers are energetically lower than the lowest-energy fusion sandwich structures by 50.3, 48.9, 48.9, 56.0, 44.0, and 50.9 kcal/mol for $\text{M} = \text{Li}, \text{Na}, \text{K}, \text{Be}, \text{Mg},$ and Ca , respectively. The lowest-energy sandwich structures are energetically higher than many fusion isomers and are thus thermodynamically unstable.

Heterodecked Sandwich-Type Compounds: $[\text{CpM}(\text{SiAl}_3)]^{q-}$ and $(\text{M}^+)_q[\text{CpM}(\text{SiAl}_3)]^{q-}$.

As known from the preceding sections, the “homodecked sandwich” form is not the ground-state structure for all six homodecked systems: $[\text{Si}_2\text{Al}_6\text{Li}]^-$, $[\text{Si}_2\text{Al}_6\text{Na}]^-$, $[\text{Si}_2\text{Al}_6\text{K}]^-$, $[\text{Si}_2\text{Al}_6\text{Be}]$, $[\text{Si}_2\text{Al}_6\text{Mg}]$, and $[\text{Si}_2\text{Al}_6\text{Ca}]$. This indicates that the all-metal aromatic SiAl_3^- cannot be used to sandwich the atoms of Li, Na, K, Be, Mg, and Ca in

(30) Jutzi, P.; Burford, N. *Chem. Rev.* **1999**, *99*, 969–990.

(31) MO pictures were made with the MOLDEN3.4 program. Schaftenaar, G. *MOLDEN3.4*, CAOS/CAMM Center: The Netherlands, 1998.

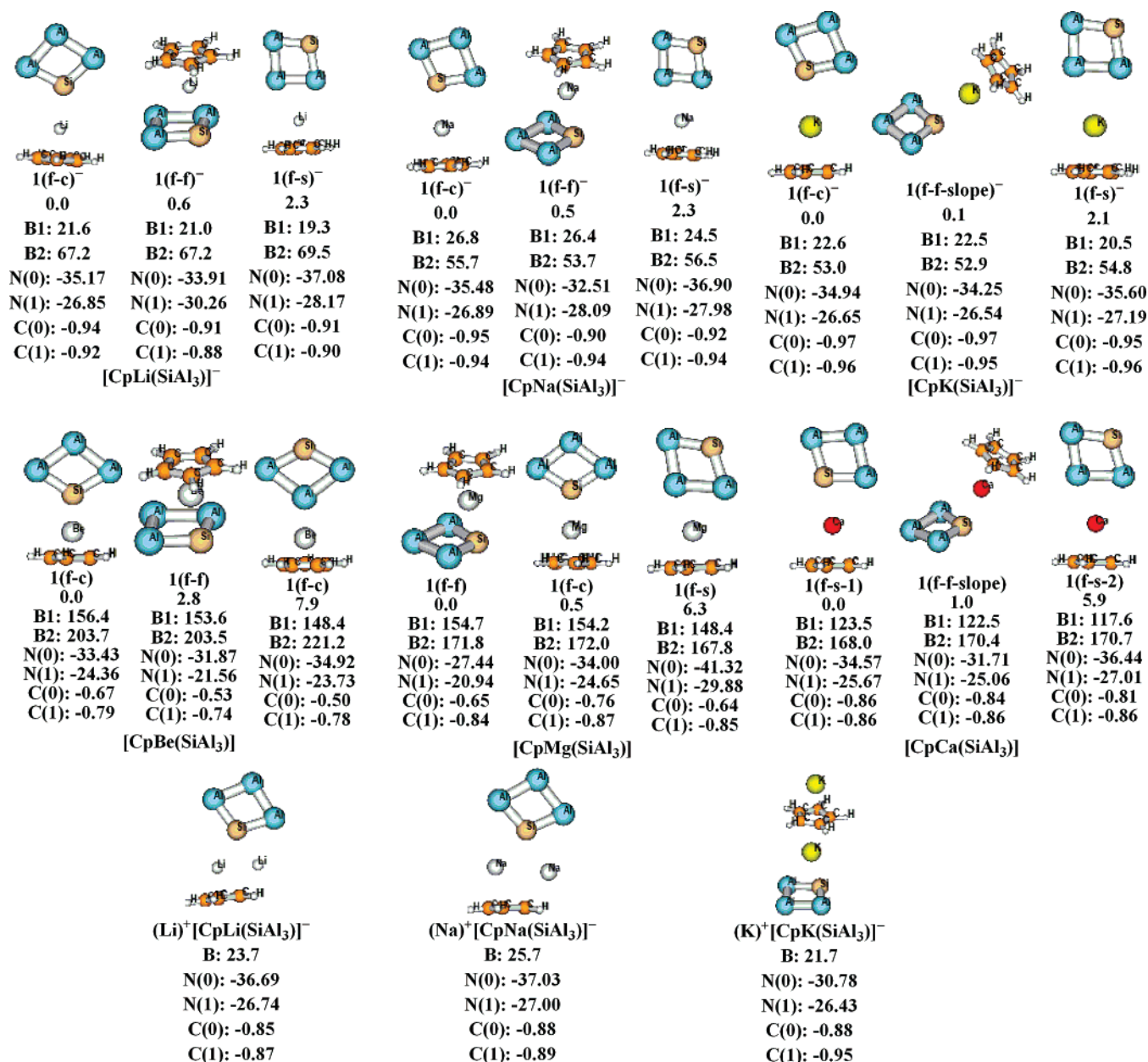


Figure 3. Low-lying sandwich forms of $[\text{CpM}(\text{SiAl}_3)]^{q-}$ ($M = \text{Li, Na, K, } q = 1$; $M = \text{Be, Mg, Ca, } q = 0$) and the lowest-energy saturated sandwich forms of $(\text{M}^+)[\text{CpM}(\text{SiAl}_3)]^-$ ($M = \text{Li, Na, K}$) obtained at the B3LYP/6-311+G(d) level. Energy values are in kcal/mol. “B(1)” denotes the binding energies between SiAl_3^- and CpM^{q+} ; “B(2)” denotes the binding energies between Cp^- and $\text{M}(\text{SiAl}_3)^{q+}$ ($M = \text{Li, Na, K, } q = 0$; $M = \text{Be, Mg, Ca, } q = 1$). “N(0) and N(1)” denote the nucleus-independent chemical shift (NICS) at the ring center and 1 Å above the ring of SiAl_3^- , respectively. “C(0)” and “C(1)” denote the natural charge distributions on the fragments SiAl_3 and Cp, respectively. “B” denotes the binding energies between CpM and $\text{M}(\text{SiAl}_3)$ in the saturated sandwich species ($M = \text{Li, Na, and K}$).

the traditional “homodecked sandwich” scheme. Here, we propose that a rigid unit such as the versatile $c\text{-C}_5\text{H}_5^-$ (Cp^-) might cooperate with the all-metal aromatic SiAl_3^- to sandwich the metal atoms M by avoidance of fusion. We call the new scheme “heterodecked sandwich”.²⁰ A new class of sandwich compounds $[\text{CpM}(\text{SiAl}_3)]^{q-}$ can then be designed. Such compounds are intuitively of special interest because they contain both the classic organic aromatic unit Cp^- and the novel all-metal aromatic SiAl_3^- .

Interestingly, the rigid organic aromatic Cp^- plays double roles (both electronic and steric) in the cluster assembly of molecular compounds. From the viewpoint of steric effects, the Cp rings are essentially spacer groups, which can effectively separate, isolate, and protect the exotic all-metal aromatic SiAl_3^- , so as to prevent the SiAl_3^- clusters’ fusion during cluster

assembly. Here, we simply call the Cp rings spacer groups to demonstrate their organometallic chemical effects in our designed heterodecked sandwich-type complexes. On the other hand, Cp rings are electron acceptors, which receive electrons donated from the metal atoms to form the closed-shell anions Cp^- , which interact with the metal atoms through electrostatic or ionic interactions. The fragments (Cp^-), (M^{q+}), and (SiAl_3^-) form sandwich compounds $[\text{CpM}(\text{SiAl}_3)]^{q-}$ by ionic electrostatic interactions. This interaction forms $(\text{Cp}^-)(\text{M}^{q+})(\text{SiAl}_3^-)$ (anions and cations alternately arranged through electrostatic interaction), can develop into highly extended 3D sandwich-like species, e.g., oligomers or polymers, which is a common phenomenon for the metalocenes of the main-group elements, especially for alkali and alkaline-earth metalocenes, that are known for a long time.

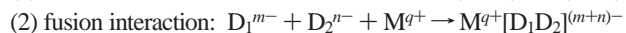
Various isomeric forms for each of the six main-group elements ($M = \text{Li, Na, K, Be, Mg, Ca}$) were searched. For simplicity, only the lower-lying sandwich structures are shown in Figure 3. Others can be found in the Supporting Information. For each alkali metal M (Li, Na, K) and each alkaline-earth metal M (Mg, Ca), there are three kinds of sandwich forms, $\mathbf{1}^q$ -(f-c), $\mathbf{1}^q$ -(f-f), and $\mathbf{1}^q$ -(f-s), with the former associated with the “face (Cp^-)–corner (SiAl_3^-)” (f-c) type and “face (Cp^-)–face (SiAl_3^-)” (f-f) type, and the latter with the “face (Cp^-)–side (SiAl_3^-)” (f-s) type. The three sandwich forms can easily convert to each other via simple rotation (the rotation frequency is very small). For alkaline-earth metal $M = \text{Be}$, there are three kinds of sandwich forms, $\mathbf{1}$ (f-c-1), $\mathbf{1}$ (f-f), and $\mathbf{1}$ (f-c-2), and one of the f-c forms is converted from the f-s form during the geometrical optimization. The three sandwich forms can easily convert to each other via simple rotation. Interestingly, among all the designed homodecked and heterodecked sandwich species, the all-metal aromatic SiAl_3^- generally prefers to interact with the partner deck SiAl_3^- or Cp^- at the side (Al–Al or Al–Si bonds) or corner (Si or Al atoms) site. First, metal atoms are likely to interact with Si atoms in the SiAl_3^- units in the heterodecked sandwich species due to its large electronegativity. Second, metal atoms are inclined to interact with Al–Al bonds in the SiAl_3^- units due to the second large negative charge distribution in Al–Al bonds. This is in contrast to the already known decks such as the famous and versatile Cp^- and the carbon-free and exotic P_5^- ,^{20a-c} Al_4^{2-} ,^{20d-f} and N_4^{2-} ,^{20g-j} which prefer the traditional face–face interaction type. Thus, the designed sandwich species in this paper represent a new kind of metallocenes. Among all the calculated $[\text{CpM}(\text{SiAl}_3)]^{q-}$ systems, the planar Cp^- structure is well-maintained, indicative of the unique “rigidity” of this organic unit. Fusion of the Cp^- and SiAl_3^- decks to form new C–Al, C–Si, or C–M bonds is energetically unfavorable. The rigid organic deck Cp^- can effectively assist the all-metal aromatic SiAl_3^- to sandwich metal atoms.

For the purpose of actual synthesis, we also designed neutral species $(\text{M})^+[\text{CpM}(\text{SiAl}_3)]^-$ ($M = \text{Li, Na, K; } q = 1$) (see Figure 3) with counterions M^+ . For each M , the lowest-lying sandwich isomer in charged $[\text{CpM}(\text{SiAl}_3)]^{q-}$ is also the ground-state structure in neutral $(\text{M})^+[\text{CpM}(\text{SiAl}_3)]^-$. Surely, the counterions have little influence on the nature of the ground-state structure. The results of the above calculation have demonstrated that the f-c, f-f, and f-s interaction types are common phenomena in the extended systems. Such an interesting growth pattern might be applicable to the assembly of Si-doped all-metal aromatic SiAl_3^- into highly extended sandwich-like compounds.

From Figure 3, we can see that the strength of the bonds $\text{Cp}^-M(\text{SiAl}_3)$ (noted as “**B2**” in Figure 3) ranges from 53 to 203 kcal/mol, and the strength of the bonds $\text{CpM}^-(\text{SiAl}_3)$ (noted as “**B1**” in Figure 3) range from 20 to 156 kcal/mol in the heterodecked sandwich-type complexes $[\text{CpM}(\text{SiAl}_3)]^{q-}$. Thus the binding energies of the Cp ring to metal atoms are larger than that of the (SiAl_3) ring to metal atoms, and the bonds $\text{Cp}^-M(\text{SiAl}_3)$ are stronger than the bonds $\text{CpM}^-(\text{SiAl}_3)$ in the heterodecked sandwich species. Such phenomena are mainly ascribed to the high stability and strong aromaticity of the closed-shell organic rigid deck Cp^- , which leads to the stability of the dissociation fragments ($\text{Cp}^- + \text{M}(\text{SiAl}_3)^{q+}$), which is higher than that of the dissociation fragments ($\text{CpM}^{q+} + \text{SiAl}_3^-$). In summary, the two kinds of ionic electrostatic interactions ($\text{Cp}^-M(\text{SiAl}_3)$ and $\text{CpM}^-(\text{SiAl}_3)$) connect the two decks Cp^- and SiAl_3^- by the bridge of metal atoms to form the heterodecked sandwich-type complexes $\text{Cp}^-M^-(\text{SiAl}_3)$.

Doping Effects in the Assembly and Stabilization of All-Metal Aromatic SiAl_3^- . In this section, we discuss the doping effects of the assembly and stabilization of Si-doped all-metal aromatic SiAl_3^- . Si-doping leads to some interesting phenomena and characteristics: (1) the number of sandwich-type forms of Si-doped SiAl_3^- is more than that of pure Al_4^{2-} , (2) the f-c (corner is Si atom) sandwich forms are low-lying structures in our designed SiAl_3^- -based sandwich-like complexes, and there is a slope of the fragment CpM in the f-f sandwich forms compared with that of pure Al_4^{2-} , (3) the gradient of the slope of CpM in the f-f sandwich forms increases from Li (Be) \rightarrow Na (Mg) \rightarrow K (Ca), due to the increasing ionic characters in the order Li (Be) \rightarrow Na (Mg) \rightarrow K (Ca). The above facts could be explained by the electrostatic interaction between CpM^{q+} and SiAl_3^- . The subunit CpM is apt to interact with the Si atom in SiAl_3^- due to the larger difference of electronegativity between M and Si atoms compared to that of M and Al atoms for the same metal atoms.

Nature and Origin of Fusion. Why can the assembly of SiAl_3^- only be realized in the form of the “heterodecked sandwich” scheme instead of the traditional “homodecked sandwich” scheme? Why would the “homodecked sandwich” assembly lead to fusion between two SiAl_3^- decks? To answer these questions, let us analyze the origin of such fusion. Intuitively, the monoanionic all-metal aromatic SiAl_3^- bears both fusion and ionic characteristics. From a combinational viewpoint, when the decks D_1^{m-} and D_2^{n-} and one M^{q+} ion are brought together, two types of reaction processes might take place, i.e.,



In process (1), each sandwich deck (D_1^{m-} and D_2^{n-}) undergoes electrostatic interaction with M^{q+} to form a sandwich-like structure $(\text{D}_1^{m-})\text{M}^{q+}(\text{D}_2^{n-})$. Process (2) is associated with the “clustering fusion”. In principle, there is a trend for any two decks to form a more coagulated cluster containing more bonds so as to lower the system energy.

The competition between processes (1) and (2) determines whether formation of a sandwich-like complex can lead to energetic stabilization or not. In the traditional “homodecked sandwich” form, the fusion interaction overwhelms the ionic interaction because of the favorable cluster coagulation. The bonding within the all-metal aromatic SiAl_3^- is not strong enough to prevent fusion. So, as shown above, the homodecked sandwich structures are energetically much less stable than the fused isomers. Yet the situation is quite different in the novel “heterodecked sandwich” form. The fusion tendency can be greatly suppressed due to the introduction of the rigid sandwiching partner Cp^- . The large organic aromaticity allows Cp^- to keep its (near) D_{5h} structure. Any fusion with SiAl_3^- will destroy the aromaticity of Cp^- and greatly raise the system energy. As a result, only in the form of the novel “heterodecked sandwich” scheme can the all-metal aromatic SiAl_3^- be assembled into sandwich-like complexes.

Extended Sandwich Structures Based on All-Metal Aromatic SiAl_3^- . It is known that some metallocenes can form highly extended sandwich complexes ranging from nanoscale structures to polymers, and even bulk solid materials.¹⁹ We thus further designed the all-metal aromatic SiAl_3^- -based extended systems containing more Cp^- and SiAl_3^- units in various heterodecked sandwich forms at the B3LYP/6-31+G(d) level. For systemic consideration, we considered various combinational forms according to different coordinated directions (face, side, and corner) of the SiAl_3^- unit. In Figure 4, some selected low-

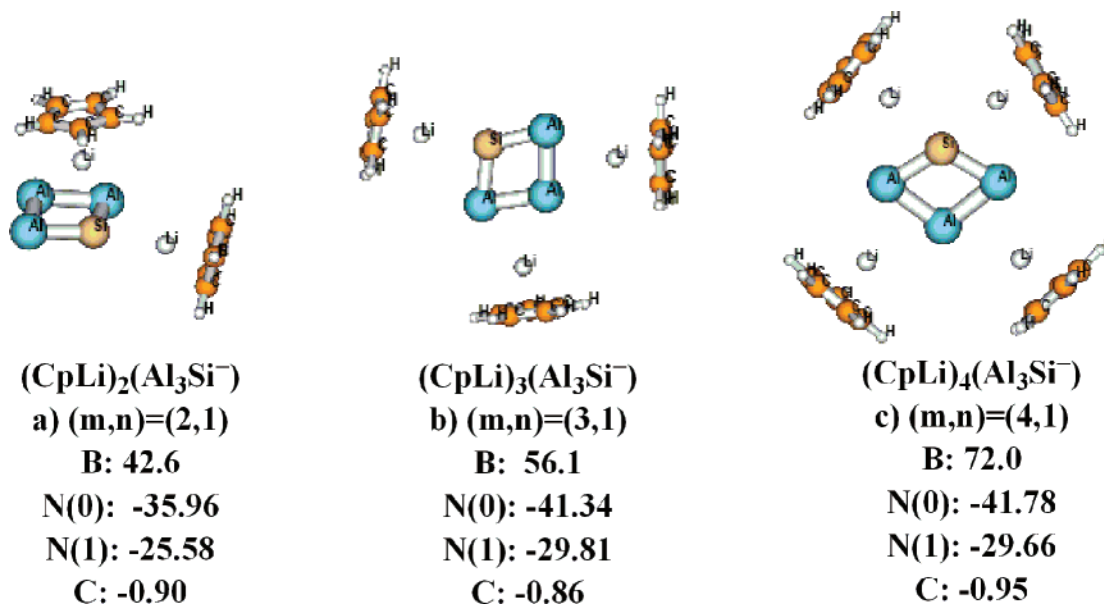


Figure 4. Low-lying extended sandwich complexes of $(\text{CpLi})_m(\text{SiAl}_3)_n$ obtained at the B3LYP/6-31+G(d) level for $(m,n) = (2,1)$, $(3,1)$, and $(4,1)$. “B” denotes the binding energies between SiAl_3^- and $m(\text{CpLi})$. “N(0) and N(1)” denote the nucleus-independent chemical shift (NICS) at the ring center and 1 Å above the ring of SiAl_3^- , respectively. “C” denotes the natural charge distributions on the fragments SiAl_3^- .

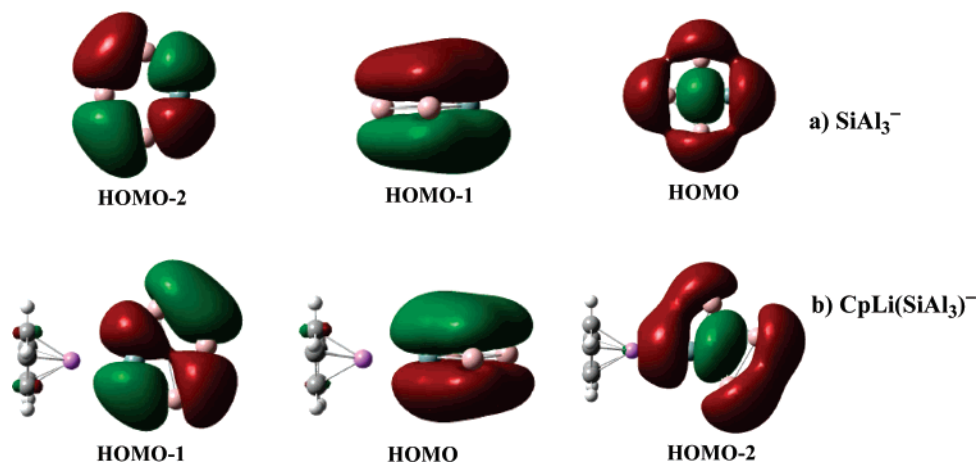


Figure 5. B3LYP/6-311+G(d) characteristic orbital diagrams³¹ of (a) $[\text{SiAl}_3]^-$ and (b) $[\text{CpLi}(\text{SiAl}_3)]^-$. The pink balls represent Li atoms, the orange balls represent Al atoms, and the light blue balls represent Si atoms. The black and white balls represent C and H atoms, respectively.

lying species are shown. Many other designed extended sandwich structures can be found in the Supporting Information.

From Figures 3, 4, and 5, we can see that the structural and electronic integrity and the orbital features of the Si-doped all-metal aromatic unit SiAl_3^- are well-maintained during the heterodecked sandwiching. Figure 5 illustrates the selected orbital diagrams of $[\text{CpLi}(\text{SiAl}_3)]^-$ as well as the comparative species SiAl_3^- . We can see that the three characteristic orbitals in the free SiAl_3^- (one delocalized π (HOMO-1) and two delocalized σ (HOMO and HOMO-2)), which contribute to the so-called “multiple aromaticity”,¹⁸ can be found in heterodecked sandwich compounds $[\text{CpLi}(\text{SiAl}_3)]^-$. A significant difference is that the HOMO, HOMO-1, and HOMO-2 orbitals in the free SiAl_3^- are moved to HOMO-2, HOMO, and HOMO-1 in $[\text{CpLi}(\text{SiAl}_3)]^-$, respectively. It should be pointed that the HOMO-2 in the $[\text{CpLi}(\text{SiAl}_3)]^-$ (HOMO in the free SiAl_3^-) plays an important role in the cluster bonding.

In order to get insight into the interactions of our designed heterodecked sandwich-type complexes, we performed detailed

NBO³² analysis. The NPA charges on the Si atoms range from -0.74 to $-1.64 |e|$ in the heterodecked sandwich-like compounds $[\text{CpM}(\text{SiAl}_3)]^-$, whereas the Al atoms bear almost no charges or slightly negative charges in the SiAl_3 unit in $[\text{CpM}(\text{SiAl}_3)]^-$. Thus, the negative charges are mainly localized at the Si atom in the subunit SiAl_3 . The Al–Al bond bears a smaller part of negative charge than that of the Si atom. The NPA charges on alkali atoms (Li, Na, and K) range from 0.79 to 0.88 $|e|$, from 0.84 to 0.90 $|e|$, and from 0.86 to 0.97 $|e|$ in $[\text{CpM}(\text{SiAl}_3)]^-$ for $M = \text{Li}, \text{Na},$ and K , respectively. For the alkaline-earth atoms, the NPA charges range from 1.28 to 1.46 $|e|$, from 1.49 to 1.63 $|e|$, and from 1.67 to 1.72 $|e|$ in $[\text{CpM}(\text{SiAl}_3)]^-$ for $M = \text{Be}, \text{Mg},$ and Ca , respectively. We can see that the NPA charges on alkali atoms (Li, Na, and K) are slightly departed from the formally positive charge of +1. For alkaline-

(32) (a) Bauernschmitt, R.; Ahlrichs, R. *Chem. Phys. Lett.* **1996**, *256*, 454. (b) Gisbergen, S. J. A. van.; Kootstra, F.; Schipper, P. R. T.; Gritsenko, O. V.; Snijders, J. G.; Baerends, E. *J. Phys. Rev. A* **1998**, *57*, 2556. (c) Matsuzawa, N. N.; Ishitani, A.; Dixon, D. A.; Uda, T. *J. Phys. Chem. A* **2001**, *105*, 4953.

earth atoms (Be, Mg, and Ca), the NPA charges are slightly departed from the formally positive charge of +2, whereas for Be, the departure is slightly larger due to its large covalent property.

Generally, the ionic electrostatic interactions usually refer to metal atoms' interaction with the negatively charged Cp ring, thus having larger M–Cp-ring distances, whereas the covalent interactions usually refer to formation of a metal atom bond connecting to one of the atoms of the Cp ring, thus having a shorter M–Cp-ring distance, which leads to a slipped-sandwich structure. The face structures of SiAl_3^- look to be displaced from the center of the ring due to the minor orbital interactions in $[\text{CpM}(\text{SiAl}_3)]^{q-}$. However, our NBO analysis has demonstrated that the fragments Cp^- , M^{q+} , and SiAl_3^- are connected mainly through electrostatic interactions to form sandwich-type complexes $\text{Cp}^-\text{M}^{q+}(\text{SiAl}_3^-)$. Additionally, the negative charges are not even distributions on the four peripheral atoms of the SiAl_3^- ring. The negative charges are mainly distributed on the Si atoms due to the larger electronegativity of Si than that of Al. Following the theorem of electrostatics, the positively charged M atoms in the fragments CpM^{q+} tend to interact with the negatively charged Si atoms in the fragments SiAl_3^- in $[\text{CpM}(\text{SiAl}_3)]^{q-}$. Thus, the corner atom Si is bonded to the metal atoms in some low-lying face–corner (f-c) sandwich-type forms $[\text{CpM}(\text{SiAl}_3)]^{q-}$. Moreover, the NBO analysis demonstrated that the positive and negative charges are dominantly positioned at the M atom and Cp unit, respectively, indicative of the major molecular formula $(\text{Cp}^-)\text{M}^{q+}(\text{SiAl}_3^-)$ ($q = 1$ for $\text{M} = \text{Li}, \text{Na}, \text{K}$ and $q = 2$ for $\text{M} = \text{Be}, \text{Mg}, \text{Ca}$). It should be noted that the deviation from the formula $(\text{Cp}^-)\text{M}^{q+}(\text{SiAl}_3^-)$ is slightly larger for $\text{M} = \text{Be}$ (the NPA charges of SiAl_3^- units in $[\text{CpBe}(\text{SiAl}_3)]$ range from -0.50 to -0.67 | e |; the NPA charges of Cp units in $[\text{CpBe}(\text{SiAl}_3)]$ range from -0.74 to -0.79 | e |) due to its large covalent property.

We are aware that quantitative bonding analysis of main-group metallocenes $[\text{ECp}_2]$ ($\text{E} = \text{Be}–\text{Ba}$) and $[\text{ECp}]$ ($\text{E} = \text{Li}–\text{Cs}$) has been disclosed by Frenking et al.³³ They concluded that for alkali-metal metallocenes, $[\text{ECp}]$ ($\text{E} = \text{Li}–\text{K}$), the dominating interactions are electrostatic (ranging from 79.6% to 86.4%, increasing from $\text{Li} \rightarrow \text{Na} \rightarrow \text{K}$), and orbital interactions exist for a minor part (ranging from 20.4% to 10.9%, decreasing from $\text{Li} \rightarrow \text{Na} \rightarrow \text{K}$). For the alkali-earth-metal metallocenes, $[\text{ECp}_2]$ ($\text{E} = \text{Be}–\text{Ca}$), the main interactions are still electrostatic (ranging from 59.2% to 76.8%, increasing from $\text{Be} \rightarrow \text{Mg} \rightarrow \text{Ca}$), and the orbital interactions still exist for a minor part (ranging from 40.8% to 23.2%, decreasing from $\text{Be} \rightarrow \text{Mg} \rightarrow \text{Ca}$). From the above data, we can see that the percentages of the orbital interactions in the alkaline-earth-metal metallocenes $[\text{ECp}_2]$ ($\text{E} = \text{Be}–\text{Ca}$) are larger than that of alkali-metal metallocenes $[\text{ECp}]$ ($\text{E} = \text{Li}–\text{K}$), due to the larger covalent properties of the alkaline-earth metals. However, for both alkali- and alkaline-earth-metal metallocenes, the interactions are mainly electrostatic. Here, following Frenking's results and on the basis of our NBO and orbital analysis, we have demonstrated that the interactions are mainly electrostatic, increasing from

$\text{Li} (\text{Be}) \rightarrow \text{Na} (\text{Mg}) \rightarrow \text{K} (\text{Ca})$, and the orbital interactions still play a minor role in the bonding interactions in our designed heterodecked sandwich-type complexes.

Aromaticity is an interesting property in the sandwich-type complexes. We thus investigated the aromaticity of our designed heterodecked sandwich-like complexes through NICS(0) and NICS(1). From Figures 3 and 4, we can see that the aromaticity (“**N(0)**” and “**N(1)**” values in Figures 3 and 4) of the SiAl_3^- units within the assembled compounds nearly amounts to -34.30 (**N(0)**) and -26.56 (**N(1)**) ppm, like that in free SiAl_3^- , suggestive of the good aromaticity-conservation in the cluster assembly. Heterodoping by the Si atom still nicely keeps the all-metal aromaticity of SiAl_3^- . This is understandable because Si and Al are neighboring elements with similar properties, so the assembly of SiAl_3^- should resemble that of Al_4^{2-} .^{20f} Thus, SiAl_3^- could act as a new type of building block or inorganic ligand in the cluster-assembled molecular compounds. To our knowledge, this is the first time that a Si-doped all-metal aromatic unit has been considered as a building block or inorganic ligand.

4. Conclusions

In summary, our work describes the first attempt to predict the incorporation of the heterodoped all-metal aromatic SiAl_3^- into assembled molecular compounds in various sandwich-like forms. Our designed sandwich-type species await future experimental verification. The designed sandwich-like species can grow into more highly extended sandwich species (in 1D, 2D, and 3D molecular or nanoscale forms) based on SiAl_3^- . Such assembly procedures could also be applied to many other group-IV-doped all-metal aromatic molecules, such as XAl_3^- ($\text{X} = \text{Ge}, \text{Sn}, \text{Pb}$). Compared to the traditional metallocene with only Cp^- decks, our designed complexes represent a new class of metallocene containing the Si-doped all-metal aromatic SiAl_3^- , among which SiAl_3^- generally prefers to use its sides (Al–Al or Al–Si bonds) or corners (Si or Al atoms) to interact with the partner deck rather than in the form of the traditional face–face interaction type for the known decks Cp^- , P_5^- , Al_4^{2-} , and N_4^{2-} . Thus, the designed sandwich species in this paper represent a new kind of metallocene. Moreover, the electronic and structural properties of SiAl_3^- are well-retained in our designed sandwich-type complexes during the cluster-assembly process, suggestive of a good building block or inorganic ligand.

Acknowledgment. This work is supported by the National Natural Science Foundation of China (Nos. 20103003, 20573046), Excellent Young Teacher Foundation of Ministry of Education of China, Excellent Young People Foundation of Jilin Province, and Program for New Century Excellent Talents in University (NCET).

Supporting Information Available: These materials include all of the molecular coordinates, total energies, molecular vibrational frequencies, and the detailed results of the NBO and NICS analysis. This material is available free of charge via the Internet at <http://pubs.acs.org>.

OM700482B

(33) For example, see: Rayon, V. M.; Frenking, G. *Chem.–Eur. J.* **2002**, *8*, 4693.